TRENDS IN SCIENCES 2026; 23(3): 12090
https://doi.org/10.48048/tis.2026.12090
RESEARCH ARTICLE

In Silico Studies of Sembukan (*Paederia scandens*) Secondary Metabolites as Anti Diabetes Against Multiple Target Protein

Matheus Prayoga Claus[1], Liony Ariantika[1], Ferry Santoso[2], Widya Dwi Aryati[3], Kunal Nepali[4] and Willy Tirza Eden[1,*]

[1]*Department of Pharmacy, Faculty of Medicine, Universitas Negeri Semarang, Central Java 50229, Indonesia*
[2]*Department of Medicine, Faculty of Medicine, Universitas Negeri Semarang, Central Java 50229, Indonesia*
[3]*Faculty of Pharmacy, Universitas Indonesia, Depok 16424, West Java, Indonesia*
[4]*Department of Pharmaceutical Sciences, Taipei Medical University, Taipei 11031, Taiwan*

([*]Corresponding author's e-mail: willytirzaeden@mail.unnes.ac.id)

Received: 28 September 2025, Revised: 6 October 2025, Accepted: 13 October 2025, Published: 15 December 2025

Abstract

Chronic hyperglycemia is a metabolic disorder caused by insufficient insulin secretion, impaired insulin action, or a combination of both. Current oral hypoglycemic agents for managing Type 2 Diabetes (T2D) act through various mechanisms of action. *Paederia scandens* L. (commonly known as *daun sembukan*) is a perennial herb that grows in open fields, thickets and along riverbanks, with a long history of use in traditional medicine systems such as Chinese and Ayurvedic medicine for treating diverse ailments, including diabetes. In this study, we investigated the antidiabetic potential of compounds from *P. scandens* by evaluating their activity against four diabetes-related protein receptors: DPP-4, SGLT-2, PTP1B and FBPase. Among the tested ligands, three compounds — cosmetin, cynaroside and compound 39 — demonstrated superior pharmacological performance in both dynamic and kinetic evaluations. These ligands exhibited the highest binding affinities and more favorable pharmacokinetic profiles compared to other candidates, highlighting their potential as promising antidiabetic agents.

Keywords: Molecular docking, Virtual screening, Secondary metabolite, *Paederia scandens*, Diabetes

Introduction

In 2015, about 9.1 million Indonesians had diabetes and the global prevalence is projected to reach 170 million by 2025, with most cases from India and China. The disease is linked to increased free fatty acid flux to the liver, leading to dyslipidemia characterized by elevated triglycerides, VLDL, small dense LDL and CETP activation that alters HDL and triglyceride particles [1].

Chronic hyperglycemia is a metabolic disorder resulting from insufficient insulin secretion, impaired insulin action, or both, leading to disturbances in the metabolism of carbohydrates, lipids and proteins – particularly in adipose tissue, skeletal muscle and the liver. If left untreated, this condition may lead to complications such as polydipsia, dysuria, weight loss, visual disturbance, coma and in severe cases, death due to ketoacidosis or hyperosmolar nonketotic syndrome [2]. Oral hypoglycemic agents used in the management of type 2 diabetes (T2D) exert their therapeutic effects through diverse mechanisms of action, each eliciting distinct physiological responses. These agents may activate or inhibit specific drug receptors to enhance insulin sensitivity, stimulate insulin secretion, inhibit glucose absorption, or suppress hepatic glucose production [3]. In advanced stages of T2D, the use of combination therapy involving two or more oral agents from different pharmacological classes – targeting multiple pathogenic mechanisms – may be necessary for effective management, as monotherapy or agents acting on a single pathway may exhibit limited efficacy [4,5].

Conventional drugs for T2D like metformin, thiazolidinediones and sulfonylureas often associated

with significant side effects include, gastrointestinal issues, increase of heart failure, fluid retention, and edema. Therefore, people start to research alternatives from plant extracts and secondary metabolites [6]. Plants are an important source of medicine, with many drugs derived from their natural products. Their therapeutic effects are mainly due to secondary metabolites such as alkaloids, flavonoids, phenolics, essential oils and polyphenols [7]. Certain medicinal plant species exhibit pharmacological activities that are associated with the presence of compounds [8]. One of plants that could have potential as antidiabetic agents is *sembukan* (*Paederia scandens*). *Paederia scandens L.*, commonly known as *daun sembukan*, is a perennial herb that typically grows wild in open fields, thickets, or along riverbanks. *P. scandens* has a long history of traditional use in various systems of medicine including Chinese and Ayurvedic medicine and employed for a wide range of ailments for several disease including diabetes [9]. Previous studies on diabetic rats have demonstrated that extracts of *P. scandens* can significantly restore blood sugar levels, with effects comparable to standard diabetic drugs [10].

Several attempts to discover new drugs for antidiabetic agents using *in silico* approach via molecular docking studies has been done previously targeting various target receptors. Four proteins that become the focus in this research are Dipeptidyl Peptidase-4 (DPP-4). Sodium-Glucose Co-Transporter 2 (SGLT-2), Protein Tyrosine Phosphatase 1B (PTP1B) and Fructose 1,6-bisphosphatase (FBPase). DPP-4 and SGLT-2 are well established drug targets in glucose regulation in Type 2 Diabetes. PTP1B and FBPase are promising targets in diabetes for different mechanisms of glucose regulation. Therefore, we picked these four targets as our drug target.

Dipeptidyl Peptidase-4 (DPP-4) was initially identified as a lymphocyte cell surface protein, also known as the T-cell activation antigen CD26. DPP-4 is a crucial target for anti-diabetic drugs due to its central role in inactivating "incretin" hormones that are vital for glucose regulation. Blocking the DPP-4 enzyme has been proven effective to ameliorate glycemia in diabetes [11].

Sodium-Glucose Co-Transporter 2 (SGLT-2) is a protein responsible for reabsorbing approximately 90% of glucose from the renal filtrate back into the bloodstream. Inhibiting the function of SGLT-2 represents an effective therapeutic strategy for the management of diabetes, as it reduces glucose reabsorption within the body. When the process is blocked, excess glucose is excreted via the urine, therefore directly lowers plasma glucose levels, leading to improvement in glycemic parameters [12].

Protein Tyrosine Phosphatase 1B (PTP1B) is a promising therapeutic target for the treatment of T2D and obesity. Although there are no approved drugs currently exist that specifically target PTP1B, it remains a major focus of research. PTP1B plays a role in cellular processes by dephosphorylating the insulin receptors. Decreased in PTP1B activity is associated with weight loss and enhanced insulin sensitivity [13].

Fructose 1,6-bisphosphatase (FBPase) is a key rate-limiting enzyme in gluconeogenesis, facilitating the conversion of non-carbohydrate precursors such as lactate and pyruvate into glucose. It catalyzes the hydrolysis of fructose-1,6-bisphosphate to fructose-6-phosphate, a critical intermediate in glucose production. FBPase is potential molecular target for regulating blood glucose levels, with its inhibitors being explored as promising candidates for the treatment of diabetes [14]. In this research, we explored the potential of *Paederia scandens* leaf secondary metabolites as anti-diabetic agents against multiple diabetes-related protein targets, namely DPP-4, SGLT-2, PTP1B and FBPase.

Materials and methods

Compounds structure preparation from *Paederia scandens L.* and reference compounds

The research began with the preparation of 80 compound structures derived from *Paederia scandens* L., based on data obtained from the reviewed literature [9]. The molecular structures were drawn using digital structure-drawing software Marvin [15]. Once all structures were finalized, the two-dimensional representations (*.mol*/.smi) were converted into three-dimensional formats (*.mol2*/.pub) using OpenBabel [16]. Reference compounds for virtual screening and molecular docking were selected based on previous studies involving the four target receptors. A total of three reference compounds were used for each target protein, as follows: PTP1B: Ertiprotafib (ERT), KQ-791 (KQ7) and 864135-09-1 (CID: 11786814, R86); DPP-4: Alogliptin (ALO), sitagliptin (SIT) and vildagliptin

(VIL); SGLT-2: Canagliflozin (CAN), dapagliflozin (DAP) and empagliflozin (EMP); FBPase: Adenosine monophosphate (AMP), CS-917 (CS9) and MB07803 (MB0)

Preparation of target protein receptors for anti-diabetic screening

The three-dimensional structures of the target protein receptors were retrieved from the RCSB Protein Data Bank (PDB). The selected structures were as follows: DPP-4 (PDB ID 2ONC), SGLT-2 (PDB ID 7VSI), PTP1B (PDB ID 2QBP), FBPase (PDB ID 2FIE). Unnecessary components such as water molecules, co-crystallized ligands and other non-essential heteroatoms were removed using AutoDockTools [17]. Subsequently, polar hydrogens were added and Kollman charges were assigned to represent partial positive and negative distribution on the protein surface.

Method validation of molecular docking

Method validation was carried out by redocking the co-crystallized ligands or predefined reference compounds using molecular docking protocol. Molecular docking was performed using the Lamarckian Genetic Algorithm (LGA), with 50 docking runs employed to verify the method is valid. Fifty docking runs are picked because it is ideal number of runs because it is most efficient showing lowest RMSD with smallest number of runs [18].

Molecular docking of compounds from *Paederia scandens L.*

Molecular docking of compounds derived from *Paederia scandens* L. was performed using AutoDock Vina [19]. Residues surrounding the binding pocket were used as a guide to define the active site of each target protein. The docking was conducted using 60×60×60 grid box. During docking, the protein residues were kept rigid, while only the rotatable bonds in the ligands were allowed to be flexible. The docking parameters were set with an exhaustiveness value of 10 and the number of predicted bindings poses also set to 10.

Data processing and visualization of ligand-receptor interactions

Following the docking simulations, analysis was conducted to evaluate the interactions between the ligands and the receptor residues. The assessment focused on binding affinity (binding energy) and the binding pose of the ligands within the receptor's active site. Subsequently, ligand-receptor interactions were visualized using BIOVIA Discovery Studio to better interpret the molecular interactions and binding conformations.

ADMET predictions and evaluation of compounds from *Paederia scandens L.*

The ADMET profiles prediction of compounds derived from *Paederia scandens* L. were analyzed using the ADMETLab 3.0 online server [20]. This tool was employed to predict the pharmacokinetic properties and potential toxicity of the selected phytochemicals through silico analysis.

Results and discussion

Preparation of secondary metabolites structure and standard comparison

The structures of secondary metabolite compounds found in *Sembukan* leaves were constructed using the MarvinSketch software. These structures were then converted into 3D PDB format and subjected to energy minimization to ensure the compounds were in a relaxed conformation. A total of 80 compounds were modelled and labelled with codes. Additionally, reference compounds that were listed in the materials were prepared for each target protein.

Table 1 Anti diabetes target receptor, Co-crystal ligand, interacting residues, dan centre coordinates of docking.

Receptors	Co-crystallized Ligand	Interacting Residues [14]	Centre Coordinates of Docking
PTP1B (2QBP)	Ligand 527	Arg45, Tyr46, Tyr47, Ala217, Lys120, Ile219, Met258, Gln262	48, 9, 2
DPP-4 (2ONC)	Ligand SY1	Glu205, Glu206, Tyr547, Trp629	−40, −20, 15
SGLT-2 (7VSI)	Ligand 7R3	Phe98, Phe453, Val95, Leu283, Tyr290, Leu84	38, 48, 45
FBPase (2FIE)	Ligand A74	Val17, Met18, Gly21, Ala24, Leu30, Met177	3, 40, 40

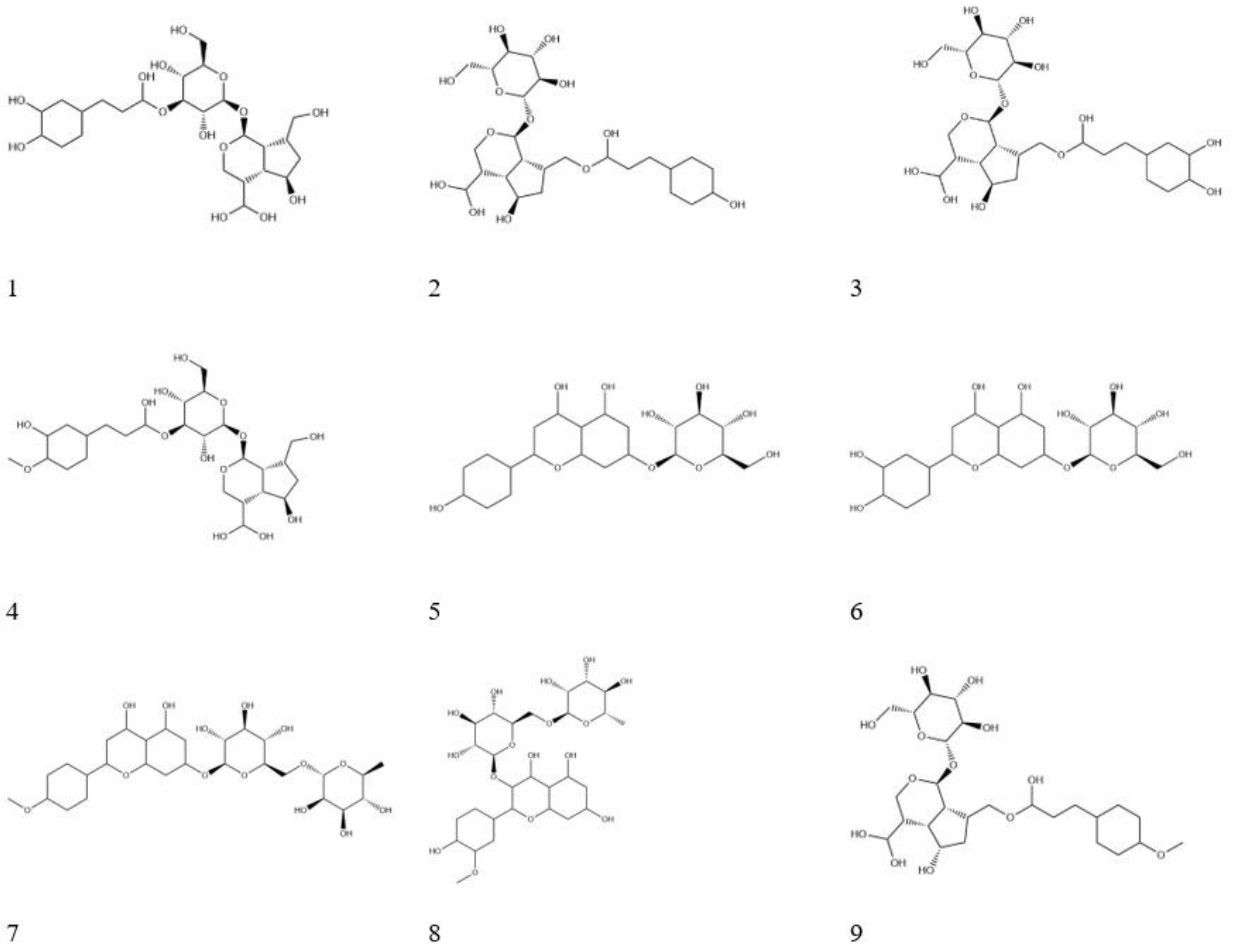

Figure 1 Chemical structures of compound 37 (1), compound 38 (2), compound 39 (3), compound 40 (4), cosmetin (5), cynaroside (6), linarin (7), narcissin (8) and paederinin (9).

Preparation of receptor protein structures and validation of the docking method

Target receptor proteins were prepared by downloading their structures from the Protein Data Bank (PDB). The structures used were PDB ID: 2QBP for PTP1B, PDB ID: 2ONC for DPP-4, PDB ID: 7VSI for SGLT-2 and PDB ID: 2FIE for FBPase. Water molecules, co-crystallized ligands and other non-essential molecules were removed using AutoDockTools. Polar hydrogens were added, and Kollman charges were assigned to represent the distribution of partial positive and negative charges. The protein structures were then saved in PDBQT format, which includes atomic coordinates, partial charges, and atom types.

The cleaned receptors were then subjected to molecular docking validation using their respective native or co-crystallized ligands to ensure optimal docking parameters. The validation process provided the coordinates for the docking site's center as follows.

Molecular docking of secondary metabolite compounds and reference compounds

All 80 compounds found in the literature are tested. Following molecular docking, we summarized the molecular docking results and picked nine ligands with the highest average binding energy. These nine compounds were selected because of their great affinity towards all four receptors. The selected compounds then analyzed further. The receptor–ligand complexes were then visualized using Discovery Studio Visualizer to examine the binding interactions and identify the interacting amino acid residues.

Table 2 Molecular docking results against PTP1B receptor.

PTP1B	Hydrogen bond	Pi-Cation Pi-Anion, Pi-Sulfur	Pi-Sigma, Pi-Alkyl	Energy binding (kcal/mol)	Estimated Ki (µM)
Compound 37	ARG254, GLY259, ARG24, GLN262, SER216	CYS215	ALA217, PHE182	–8.1	1.142
Compound 38	ASP48, ARG24, GLN262, ARG221, ARG47	-	CYS215, ALA217	–8.2	0.965
Compound 39	GLN262, ARG47, ARG221, CYS215, ASP48	-	ALA217	–7.9	1.601
Compound 40	GLY259, TYR46	-	ALA217, PHE182, ARG221, CYS215	–8.1	1.142
Cosmetin	GLN262	-	ALA217	–8.7	0.415
Cynaroside	CYS215, ARG221, ASP48, GLN262, GLY259, ARG24, TYR20, ARG254, SER216	-	ALA217, TYR46	–8.9	0.296
Linarin	ARG254, SER28, SER216, ASP29	-	TYR46, PHE182, ALA217	–8.8	0.350
Narcissin	SER118, ARG221, SER216, TYR46	-	LYS120, ALA217	–8.5	0.581
Paederinin	ASP29, ASP48, GLN262. ARG254, SER216	-	PHE182, TYR46, CYS215, ALA217	–8.2	0.965
Ertiprotafib (ERT)	ARG24, TYR46	CYS215, ARG221, MET258	ALA217, VAL49, PHE182	–8.6	0.491

PTP1B	Hydrogen bond	Pi-Cation Pi-Anion, Pi-Sulfur	Pi-Sigma, Pi-Alkyl	Energy binding (kcal/mol)	Estimated Ki (μM)
KQ-791 (KQ7)	ARG221, GLN266, GLN262, GLY220, PHE182,	-	LYS120, VAL49, ALA217	–9.2	0.178
864135-09-1 (R86)	LYS120, CYS215, ARG221, PHE182	ARG254, SER216	ALA27, ALA217	–8.3	0.815

According to the molecular docking results from the secondary metabolites of Paederia scandens, we got top 9 ligands that form good binding with the four receptors. The ligands are compound 37, compound 38, compound 39, compound 40, cosmetin, cynaroside, linarin, narcissin and paederinin.

The docking results against PTP1B showed that the ligands bind with high energy binding and low inhibition constant (–7.9 kcal/mol or 1.60 μM to –8.9 kcal/mol or 0.296 μM) with cynaroside (–8.9 kcal/mol, 0.296 μM), linarin (−8.8 kcal/mol, 0.35 μM), cosmetin (–8.7 kcal/mol, 0.415 μM), narcissin (–8.5 kcal/mol, 0.581 μM) and paederinin (–8.2 kcal/mol, 0.965 μM) being in the upper side, indicating a promising candidate for PTP1B inhibitor.

According to Liu *et al*. [21]; Ala *et al*. [22] there are 4 sites that play an important role in inhibition of PTP1B namely main catalytic “A Site” and three additional secondary sites were named B, C and D sites. Together these four sites constitute attractive structural cavities for inhibitors. The A site is from residues PHE182 to CYS215 and TYR46 to GLN262 with main residues are CYS215, GLN262, ASP181 and ARG221. Meanwhile the B site that was discovered by [23], involves residues like TYR20, ARG24, ALA27, PHE52, ARG264 and MET258-GLY259 and contributes to substrate binding and specificity. C Site consists of TYR46, ARG47 and ASP48, while D Site consists of TYR46, GLU115, LYS120, ASP181 and SER216.

KQ-791 with the highest energy binding from the three reference standards. It exhibits hydrogen bonds with ARG221, GLN266, GLN262, GLY220, PHE182, SER216 and hydrophobic interactions with LYS120, TYR46, VAL49, and ALA217 (**Figure 2(L)**). This simultaneous engagement with the main site and the secondary site provides a high bar for potency and structural template for dual site occupancy, meanwhile ertiprotafib and R86 still have great contact with the receptors but fewer than KQ-791 (**Figures 2(J)** and **2(K)**).

Several of the ligands exhibit binding to these residues. Cynaroside exhibits multiple hydrogen bonding networks to CYS215, ARG221, ASP48, GLN262, GLY259, ARG24, TYR20, ARG254 and SER216 which make cynaroside interacting almost in every main site and make the binding between the cynaroside and PTP1B greater than other ligand (**Figure 2(F)**). Linarin also forms multiple hydrogen bonds with ARG254, Ser28, Ser216 and ASP29 and π interactions with TYR46, PHE182 and ALA217. Although it lacks direct contact with the main A site, specifically CYS215 or ARG221, strong hydrophobic interactions with TYR46 or PHE182 seem to compensate for it, hence it still has strong interactions with the PTP1B receptor (**Figure 2(B)**).

Cosmetin which only exhibit 2 interactions, one hydrogen bond with GLN262 and one hydrophobic interaction with ALA217 seems adequate to hold the binding of the ligand with the receptor (**Figure 2(E)**).

Narcissin has good hydrogen bonds toward several residues which are SER11, ARG221, SER216 and TYR46 (**Figure 2(H)**) while paederinin also exhibit hydrogen bonds with ASP29, ASP48, GLN262, ARG254 and SER216 which could indicate their potential as well as PTP1B inhibitors (**Figure 2(I)**). From these results, we can proceed to conclude that cynaroside, linarin, cosmetin and narcissin are promising PTP1B inhibitors.

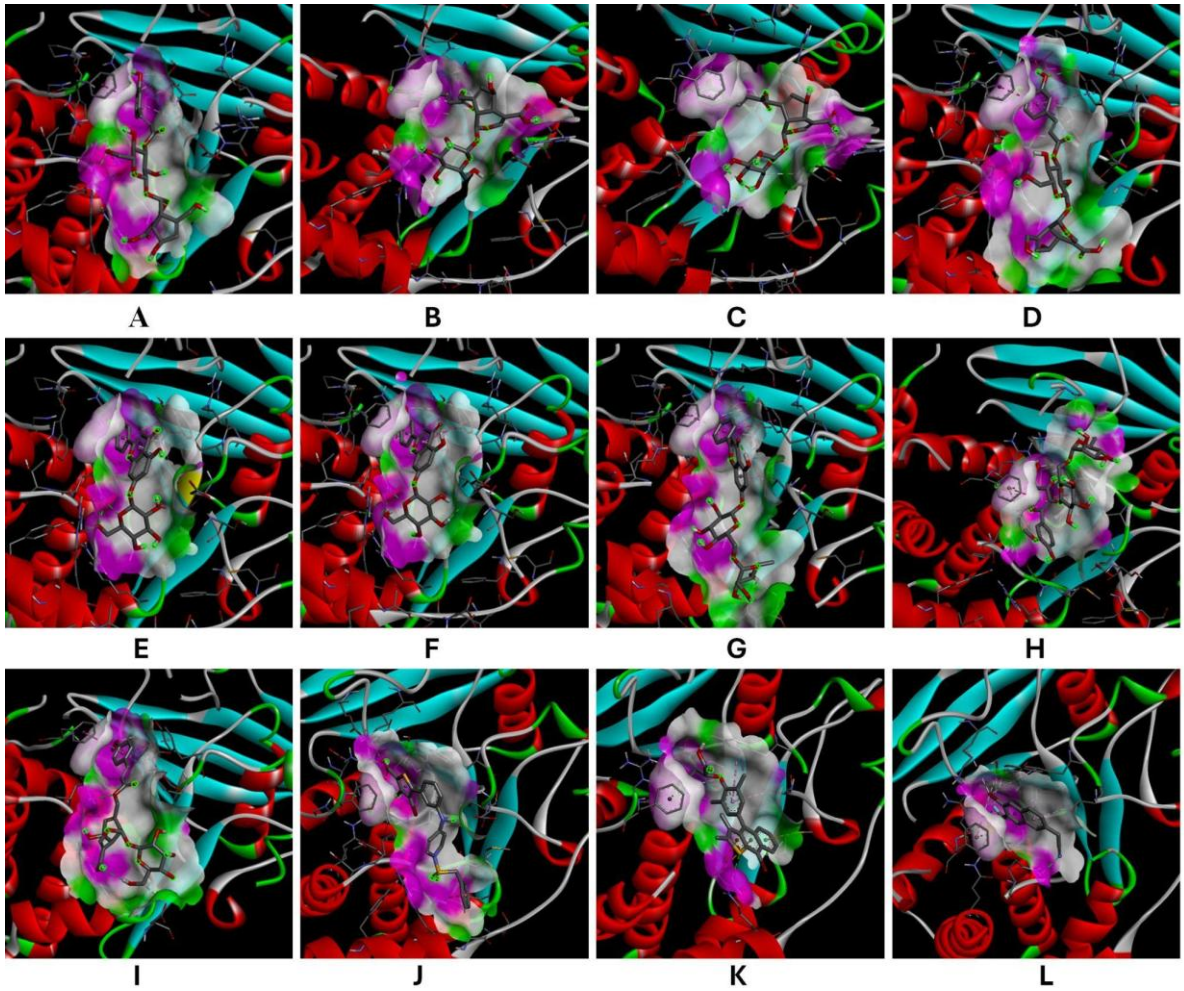

Figure 2 Interactions between PTP1B obtained from molecular docking with (A) Compound 37, (B) Compound 38, (C) Compound 39, (D) Compound 40, (E) Cosmetin, (F) Cyanaroside, (G) Linarin, (H) Narcissin, (I) Paederinin, (J) R86, (K) Ertiprotafib, (L) KQ791.

Table 3 Molecular Docking Results against DPP-4 Receptor.

DPP-4	Hydrogen bond	Pi-Cation, Pi-Anion Pi-Sulfur, Halogen	Pi-Sigma, Pi-Alkyl	Energy binding	Estimated Ki (µM)
Compound 37	PRO159, TRP157, TRP216, PRO218	-	-	–11.7	0.003
Compound 38	TRY547, HIS740, TYR585, GLU205	-	PHE357	–11.0	0.009
Compound 39	TYR631, TYR547, GLU206, SER630, HIS740	-	PHE357	–12.1	0.001
Compound 40	ASN710, TYR662, GLU205, ARG669, HIS126	-	-	–12.1	0.001
Cosmetin	HIS592, SER349, ASP588, ASN377	-	-	–10.8	0.012
Cynaroside	ASP737, ASP192, ARG253	ASP739	PHE240, VAL252, LYS122	–11.2	0.006
Linarin	TYR631, ARG358	GLU206	VAL656, TYR662, TYR666, PHE357	–11.6	0.003

DPP-4	Hydrogen bond	Pi-Cation, Pi-Anion Pi-Sulfur, Halogen	Pi-Sigma, Pi-Alkyl	Energy binding	Estimated Ki (μM)
Narcissin	ARG253, ASP192, GLN124, THR199	-	PHE240	–12.4	0.001
Paederinin	TRP629, ASP739	ARG125	HIS740	–11.1	0.007
Alogliptin (ALO)	ASP739, GLN123	-	PHE240, VAL252, ALA707	–8.8	0.350
Sitagliptin (SIT)	SER209, HIS740, TYR662	GLU206, VAL207	PHE357, TYR666	–10.2	0.033
Vildagliptin (VIL)	GLU205, ARG125, ASN710	TYR547	-	–8.8	0.350

The molecular docking results of ligands against DPP-4 Receptor shows that the energy binding of ligands varies between –12.4 to –10.8 kcal/mol, which all of them show stronger energy than the reference drugs, which are alogliptin (–8.8 kcal/mol, 0.35 μM), sitagliptin (–10.2 kcal/mol, 0.033 μM), and vildagliptin (–8.8 kcal/mol, 0.350 μM). Narcissin, compound 39 and compound 40 showed the best binding energies (< –12.0 kcal/mol), while compound 37, linarin, cynaroside, and paederinin followed them.

As we already know previously that the catalytically critical or recognition residues in the table include region with saline bridging residues such as GLU205, GLU206 and TYR662; S1 and S2 regions which contain ARG125, SER209, PHE357, ARG358, TYR547, SER630, TYR666 and ASN710; other important sites such as ASP192, VAL207 and ARG253 which are essential for substrate recognition and catalysis [24-27]. Besides those residues, other interacting residues such as PHE240, VAL252 and ALA707 also play important roles in the binding of ligands to the receptors [28].

The secondary metabolites show great potential for inhibition of DPP-4 activity, and each with their own mechanism which could be described to 2 main categories. Compound 38, compound 39, compound 40, paederinin and linarin for example exhibit binding to ARG125 / GLU205 / GLU206 / PHE357 / TYR662 which is very similar to the model of vildagliptin and sitagliptin binding to the receptor. Compound 40 (**Figure 3(D)**) is especially shown in this result like vildagliptin (**Figure 3(K)**) in the mode of binding, which is to GLU205 (anchor) and ASN710 (S1 floor).

Meanwhile cynaroside and narcissin binding to ASP192 and ARG253 residues. These residues are located near the entrance/interface and can contribute to polar anchoring (**Figures 3(F)** and **3(H)**). PHE240 and VAL252 are hydrophobic and provide affinity improvement.

Compound 37 on the other hand has bonding to PRO159, TRP157, TRP216 and PRO218, which are peripheral to S1/S2 pocket and indicate binding near a surface loop or entry channel rather than deeply filling S1 or S2 as is shown in **Figure 3(A)**. The result is a reasonable docking score and stabilized mainly by shape complementarity rather than pharmacophore interactions. Overall, cynaroside, narcissin, linarin, compound 39 and compound 40 could be candidates for inhibiting the activity of DPP-4 receptor.

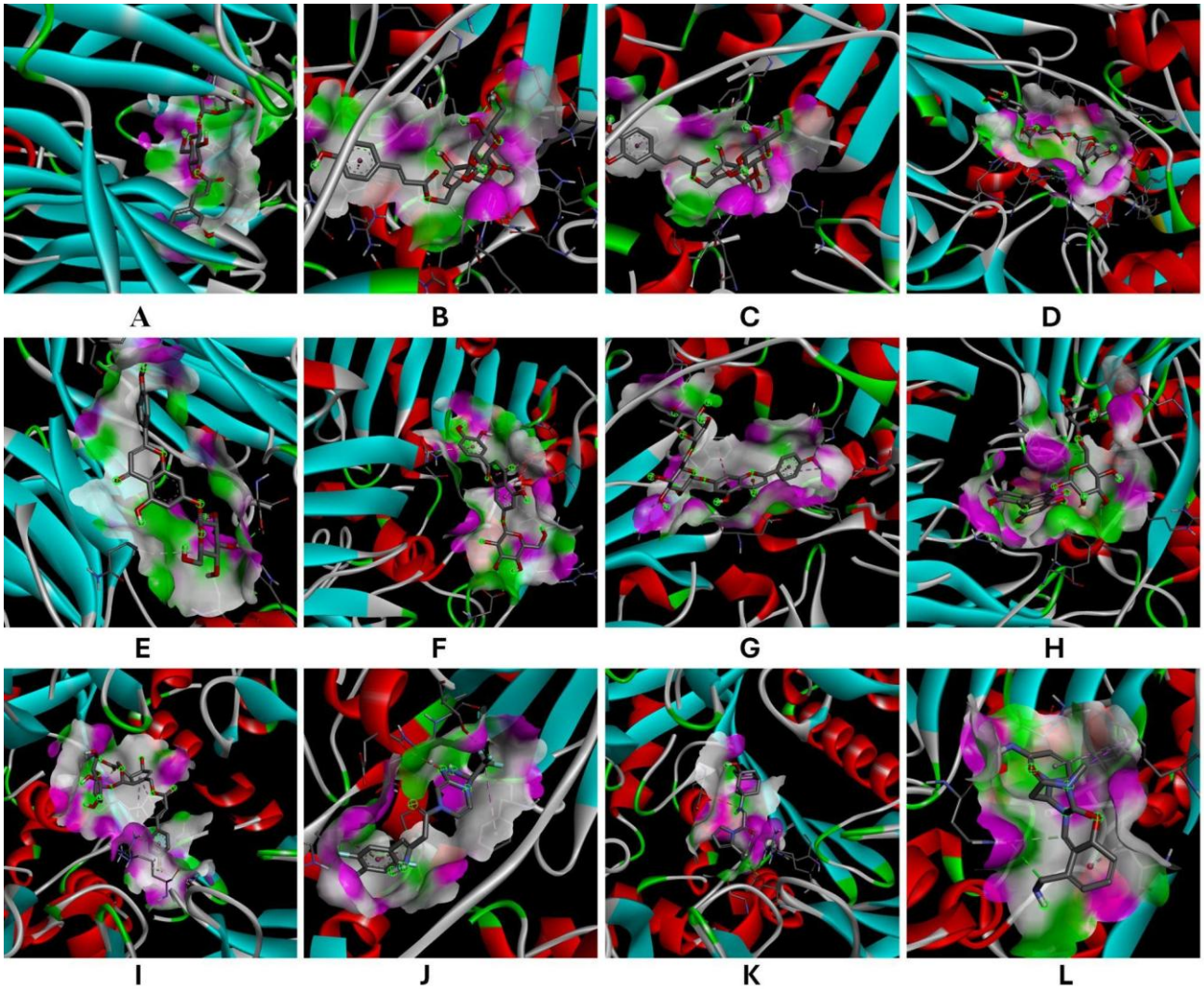

Figure 3 Interactions between DPP-4 obtained from molecular docking with (A) Compound 37, (B) Compound 38, (C) Compound 39, (D) Compound 40, (E) Cosmetin, (F) Cyanaroside, (G) Linarin, (H) Narcissin, (I) Paederinin, (J) Sitagliptin, (K) Vildagliptin, (L) Alogliptin.

Table 4 Molecular Docking Results against SGLT-2 Receptor.

SGLT-2	Hydrogen bond	Pi-Cation, Pi-Anion Pi-Sulfur	Pi-Sigma, Pi-Alkyl	Energy binding (kcal/mol)	Estimated Ki (μM)
Compound 37	PHE98, GLU99, GLN457, ASN75, SER393, SER74	ASP158	LYS154, VAL157	–10.7	0.014
Compound 38	GLN457, ASN75, HIS80	-	PHE98, VAL95, PHE453	–9.9	0.055
Compound 39	ASN75, LYS154, ASP158, TYR290, HIS80	-	PHE98, VAL95, PHE453	–9.8	0.065
Compound 40	SER460, GLN457, ASP158, HIS80, SER74, PHE98, TYR290	-	VAL157, LYS154, ILE397	–10.5	0.020
Cosmetin	THR87, ASN75, GLN457, SER287	HIS80	VAL95, PHE453, VAL157	–10.5	0.020

SGLT-2	Hydrogen bond	Pi-Cation, Pi-Anion Pi-Sulfur	Pi-Sigma, Pi-Alkyl	Energy binding (kcal/mol)	Estimated Ki (μM)
Cynaroside	THR97, ASN75, GLU99, HIS80	-	VAL95, PHE98, PHE453, VAL157	–10.4	0.023
Linarin	TYR290, ASN75, LYS154, GLY79, GLN457, THR153, HIS80, GLY83	GLU99	VAL95, LEU84, PHE98, PHE453, LEU274, ILE397	–9.7	0.077
Narcissin	GLY79, ASP454, GLN457	HIS80	VAL157, TYR290	–9.2	0.178
Paederinin	HIS80, SER460, GLN457, PHE98, GLU99	ASP454	-	–9.9	0.055
Canagliflozin (CAN)	GLU99	PHE98, ASP454	HIS80, LEU84, VAL95, PHE453	–10.9	0.010
Dapagliflozin (DAP)	GLN457, HIS80, PHE98, TRP291	-	LEU84, VAL95, LEU274	–10.2	0.033
Empagliflozin (EMP)	LYS321, PHE98, TYR526	HIS80, GLY79	VAL95, LEU84, LEU274	–11.2	0.006

Molecular docking results for ligands against SGLT-2 receptors were found as shown in **Table 4**. Binding energies and Ki for the ligands ranged from –9.2 kcal/mol, 0.178 μM to –10.7 kcal/mol, 0.014 μM while the reference used also showed good energy binding with canagliflozin (–10.9 kcal/mol, 0.01 μM), dapagliflozin (–10.2 kcal/mol, 0.033 μM) and empagliflozin (–11.2 kcal/mol, 0.006 μM). The three reference drugs are used because they are in line with their known high potency as clinical SGLT-2 inhibitors [29].

Previous study showed that ASN75, HIS80, LYS154, TYR290, TRP291, PHE453 and ILE456 to be important residues in the binding of ligands to SGLT-2 receptor [30]. Compound 37 with the lowest binding energy form binding with ASN75 and LYS154 residues which is important for binding with the receptor. Moreover, it also binds to PHE98, VAL157 and GLN457 which seems to be the common residues too with the other mode of binding from other ligands (**Figure 3(A)**).

Compound 40 exhibits multiple hydrogen bonds toward the receptor with HIS80 and TYR290 as the main residues. This suggests that compound 40 anchors to the polar rim and inserts toward the mid region of the pocket (**Figure 4(D)**). Cosmetin with similar binding energy with compound 40 exhibits binding with ASN75 in hydrogen bonding and HIS80 and PHE453 as hydrophobic interactions (**Figure 4(E)**). Similarly to cosmetin is cynaroside which has hydrogen bonding toward ASN75 and HIS80 while PHE453 interacts hydrophobically (**Figure 4(F)**).

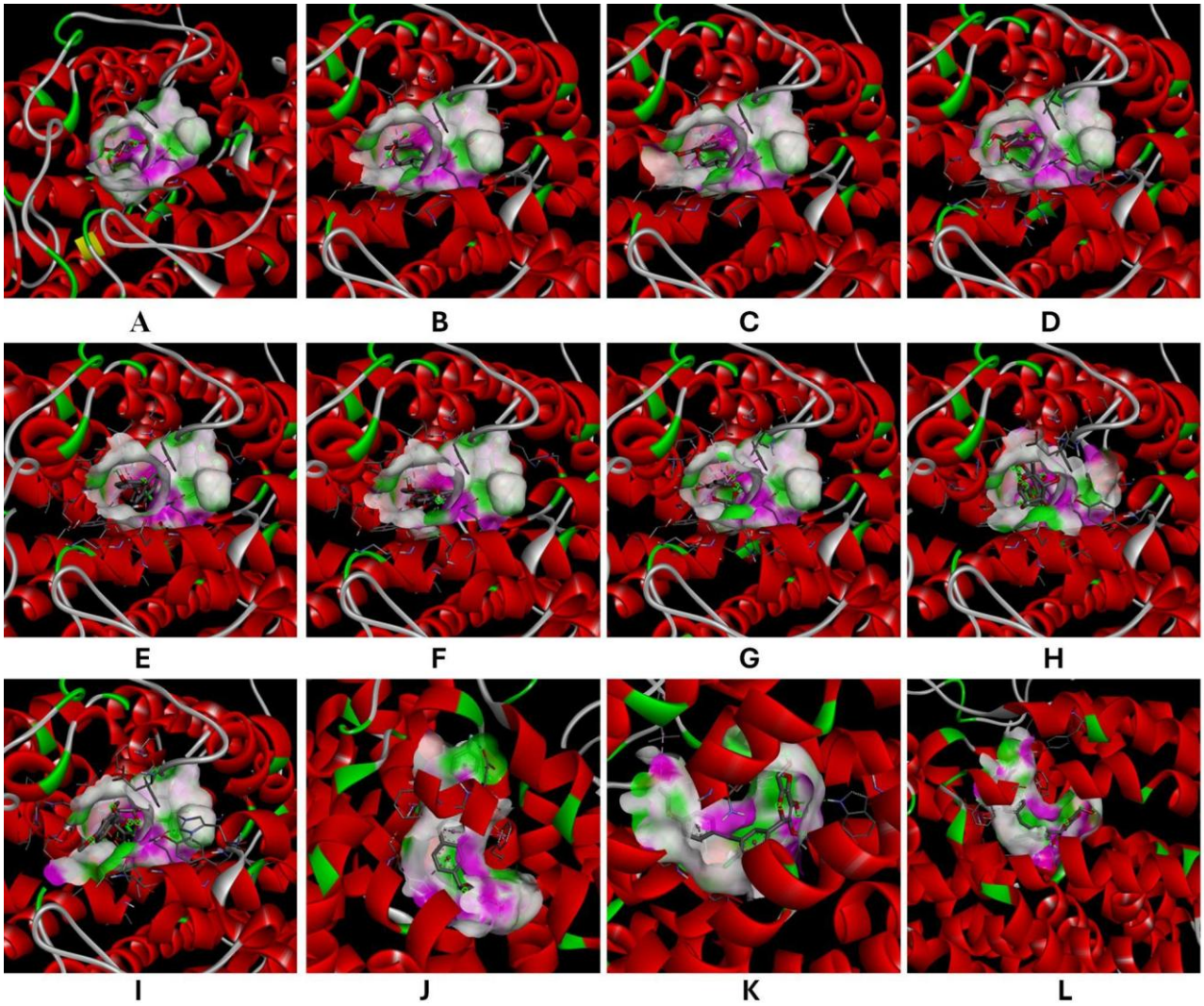

Figure 4 Interactions between SGLT-2 obtained from molecular docking with (A) Compound 37, (B) Compound 38, (C) Compound 39, (D) Compound 40, (E) Cosmetin, (F) Cyanaroside, (G) Linarin, (H) Narcissin, (I) Paederinin, (J) Canagliflozin, (K) Dapagliflozin, (L) Empagliflozin.

Table 5 Molecular Docking Results against FBPase Receptor.

FBPase	Hydrogen bond	Pi-Cation, Pi-Anion, Pi-Sulfur	Pi-Sigma, Pi-Alkyl	Energy binding (kcal/mol)	Estimated Ki (μM)
Compound 37	GLY26, THR31, THR27, ARG22	-	-	–8.4	0.688
Compound 38	THR27	-	ARG22, GLY21	–8.2	0.965
Compound 39	ARG22, THR31, GLY26, ARG25, GLY28, THR27	-	ARG22, GLY21	–8.6	0.491
Compound 40	THR31, GLY26, GLU19	-	ARG22	–8.4	0.688
Cosmetin	GLY26, MET18, GLY21, GLY28	ARG22	ARG25	–8.2	0.965
Cynaroside	GLY26, MET18, THR27	-	ARG25	–8.3	0.815

FBPase	Hydrogen bond	Pi-Cation, Pi-Anion, Pi-Sulfur	Pi-Sigma, Pi-Alkyl	Energy binding (kcal/mol)	Estimated Ki (μM)
Linarin	ARG22, THR31, ARG25, THR27, GLY26, GLY28, GLY21	-	PHE89	–9.6	0.091
Narcissin	GLY21, GLY26, GLY28, GLY28, ARG25	-	MET1, ARG22, ARG25	–8.6	0.491
Paederinin	GLY29, THR27, THR31, ARG22, GLY21, GLY26, GLU20	-	ALA24	–8.7	0.415
Adenosine monophosphate (AMP)	MET18, GLY26, GLY28, THR31	-	ARG22, ARG25	–7.3	4.412
CS-917 (CS9)	THR27, ARG22	-	ARG25, ARG22	–7.6	2.658
MB07803 (MB0)	ARG22, THR27, GLY28	-	ARG25	–8.7	0.415

Our molecular docking results of ligands against the FBPase receptor show various energy binding and Ki ranging from –8.2 kcal/mol, 0.965 μM to –9.6 kcal/mol, 0.091 μM. Among all compounds, linarin demonstrated the most favorable binding (–9.6 kcal/mol, 0.091 μM) surpassing all references.

Previous research found that several residues that interact with the ligand in the bonding pocket site of FBPase are THR27, GLY28, GLU29, LYS112, TYR113, GLY21, ARG22, GLY26, THR31, ARG140, VAL160, MET177, ASP178, and CYS179 [31]. From the results we can conclude that GLY21, ARG22, GLY26, THR27, GLY28 and THR31 form frequent hydrogen bonding toward almost all the ligands. Compound 39 and Linarin engaged with ARG22, THR31, GLY26, GLY28, and THR27 simultaneously, suggesting a stabilizing interaction network within this pocket (**Figures 5(C)** and **5(G)**).

We can also see that almost all the ligands have hydrophobic interactions with ARG22 and ARG25. This could be a highlight that ARG22 is a recurrent 'anchoring' residue, crucial for ligand orientation within the binding site, since this residue is interacting with many ligands except linarin, which interacts with PHE89. Even though it doesn't interact with ARG22 or ARG25, it achieved the lowest inhibition constant (0.091 μM). This could potentially show that flavonoid scaffolds with extended aromatic systems may exploit both polar and hydrophobic interactions in the binding pocket [32]. In this case, we could conclude that linarin, paederinin, or narcissin could be the best candidate for FBPase inhibitor.

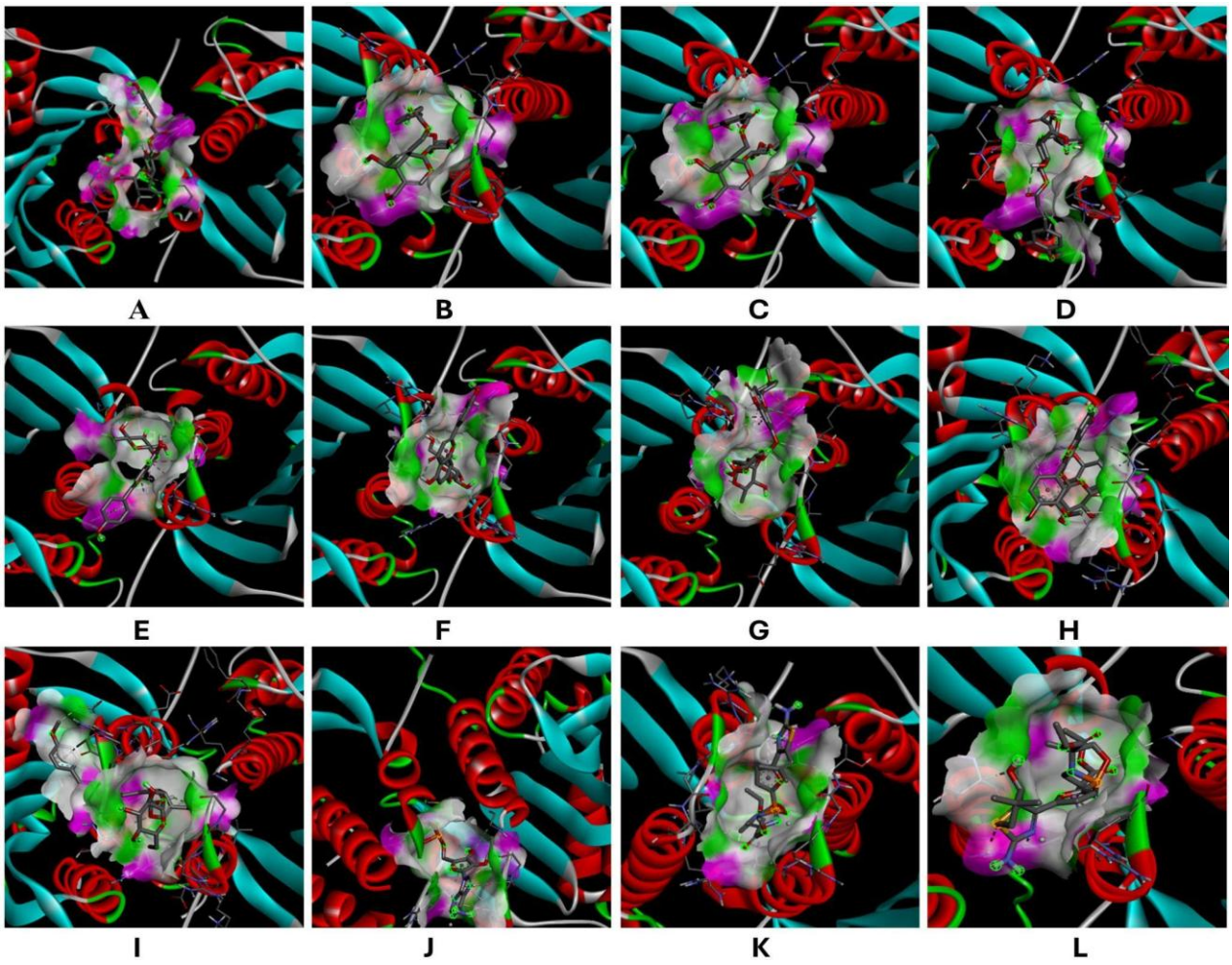

Figure 5 Interactions between FBPase obtained from molecular docking with (A) Compound 37, (B) Compound 38, (C) Compound 39, (D) Compound 40, (E) Cosmetin, (F) Cyanaroside, (G) Linarin, (H) Narcissin, (I) Paederinin, (J) Adenosine monophosphate, (K) CS9, (L) MBO.

ADMET Predictions

Table 6 showed the ADMET prediction of 9 top secondary metabolites of Paederia scandens. Molecular weight properties of most compounds are over 500 Da, which may reduce oral bioavailability [33]. Cosmetin and Cynaroside are within the favorable range.

For the number of hydrogen bond acceptors (nHA), cosmetin and cynaroside are within the acceptable range (≤ 10 ideally). Higher numbers of hydrogen bonds acceptor may reduce the permeability of molecules inside the body [34]. No ligand is fulfilling the number of hydrogen bonds donors, since it is all more than 5. Cosmetin has the lowest number of hydrogen bonds donors. All compounds also have negative (< 0) logP, which means that they are hydrophilic. This may help solubility, but it will reduce membrane permeability. From the general drug-likeness prediction, cosmetin and cynaroside are leading the table.

From the absorption aspects, all ligands have low and negative values, which is less than –5, this could mean low intestinal permeability. It is shown that all ligands have the value of Pgp inhibitor equals 0. This means that none of the ligands inhibit Pgp proteins. This is a positive result, since none of the candidates will interfere with the work of Pgp proteins in the body, which could lead to increase in bioavailability and brain penetration. However, almost all show values of Pgp substrate close to 1, which indicates that they are strong Pgp substrates. This will lead to molecules of drugs effluxing out of cell, reducing absorption.

For the distribution properties, all ligands show negative value, which indicates low tissue distribution.

This means, the ligands are mostly confined to plasma, hence lower dose of a drug is required to achieve a given plasma concentration. Blood-Brain Barrier penetration prediction also shows very low value for most (< 0.3). Only compound 38 (0.284) shows light potential. But overall, these ligands don't cross the BBB.

In the metabolism parameter, all the ligands have values almost or equal to zero which means that neither of the ligands are a substrate of CYP2D6 or CYP3A4 which could decrease the bioavailability in the body [35]. Also, none of the ligands inhibit the activity of CYP2D6 and CYP3A4. This means that it won't interact with drugs that are metabolized by the CYP2D6 and CYP3A4.

Excretion properties of the ligands showed various results, but still in the low region, which means it removes from the body slowly, with longer systemic retention. Linarin's negative value suggests that it is removed very slowly and could be retained in the body.

Most compounds display moderate half-lives with linarin and narcissin showing the longest retention time, potentially prolonging the pharmacological action but also raising the risk of toxicity.

Toxicity properties of the ligands showed mixed results of each ligand. All compounds show relatively low values (<0.1) indicating minimal risk of cardiotoxicity. Several ligands show mutagenicity risk from the AMES toxicity prediction, with compound 40, linarin, and paederinin show higher value. All ligands also showed very low carcinogenicity. Some ligands like compound 37, compound 40 and paederinin also show higher hepatotoxicity. All tested ligands also predicted to have extremely low probability of drug-induced neurotoxicity, meaning neurotoxicity is not a major concern.

Table 6 Prediction of Drug likeness and ADMET.

Parameter	Compound 37	Compound 38	Compound 39	Compound 40	Cosmetin	Cynaroside	Linarin	Narcissin	Paederinin
MW	568.27	552.28	568.27	582.29	448.23	464.23	608.3	640.29	566.29
nHA	14	13	14	14	10	11	14	16	13
nHD	10	9	10	9	7	8	8	10	8
logP	–1.98	–1.859	–2.75	–1.609	–1.206	–2.117	–1.015	–2.099	–0.544
Absorption									
Caco-2 Permeability	–5.745	–5.778	–6.173	–5.65	–6.368	–6.629	–5.829	–6.147	–5.588
Pgp inhibitor	0.0	0.0	0.0	0.0	0.0	0.0	0.0	0.0	0.0
Pgp substrate	0.997	0.99	0.987	0.999	0.945	0.951	0.883	0.999	0.882
Distribution									
VDss	–0.651	–0.58	–0.687	–0.684	–0.433	–0.462	–0.496	–0.607	–0.613
BBB	0.003	0.284	0.158	0.003	0.137	0.041	0.002	0.001	0.062
Metabolism									
CYP2D6 Substrate	0.001	0.0	0.0	0.004	0.0	0.0	0.0	0.0	0.008
CYP2D6 Inhibitor	0.0	0.0	0.0	0.0	0.0	0.0	0.0	0.0	0.0
CYP3A4 Substrate	0.0	0.0	0.0	0.0	0.0	0.0	0.001	0.004	0.0
CYP3A4 Inhibitor	0.0	0.0	0.0	0.0	0.0	0.0	0.0	0.0	0.0
Excretion									
Cl_{plasma}	2.724	1.684	1.087	1.823	1.746	0.856	0.643	–0.007	1.884
$T_{1/2}$	3.591	2.744	3.057	3.199	3.479	3.906	3.713	4.813	2.528
Toxicity									
hERG blockers	0.021	0.017	0.016	0.019	0.061	0.06	0.076	0.023	0.028
AMES toxicity	0.139	0.484	0.509	0.789	0.413	0.426	0.687	0.773	0.755
Carcinogenicity	0.066	0.02	0.018	0.092	0.051	0.05	0.017	0.007	0.054

Parameter	Compound 37	Compound 38	Compound 39	Compound 40	Cosmetin	Cynaroside	Linarin	Narcissin	Paederinin
Human Hepatotoxicity	0.707	0.553	0.526	0.758	0.596	0.593	0.355	0.356	0.637
Drug-induced Neurotoxicity	0.014	0.003	0.004	0.014	0.024	0.035	0.004	0.003	0.003

Conclusions

We have shown you the results of our studies which indicate that some of the secondary metabolites from Paederia scandens could be used in inhibiting diabetes correlated protein, whether it is by inhibiting PTP1B, DPP-4, SGLT-2 or FBPase protein with their own mechanism of action. We also showed the prediction of pharmacokinetics from each of top potential ligands. We could see the potential of 3 ligands that really showed their pharmacological performance, whether the dynamic part or the kinetic part. These three ligands are cosmetin, cynaroside, and compound 39. These 3 ligands show highest binding energy from all the ligands and pharmacokinetically better than the other ligand with high binding energy.

Acknowledgements

This research is being funded by Lembaga Penelitian dan Pengabdian kepada Masyarakat UNNES through Dana DPA Fakultas Kedokteran UNNES Tahun 2025 with Contract Number: 31.25.4/UN37/PPK10/2025.

Declaration of Generative AI in Scientific Writing

The authors acknowledge the use of generative AI tools (e.g., QuillBot) in the preparation of this manuscript, specifically for language editing and grammar correction. No content generation or data interpretation was performed by AI. The authors take full responsibility for the content and conclusions of this work.

CRediT Author Statement

Matheus Prayoga Claus: Conceptualization, Methodology, Software, Validation, Investigation, Writing – Original Draft, Writing – Review and Editing, Visualization, Supervision, and Project Administration, Funding Acquisition; **Liony Ariantika:** Investigation, Formal Analysis, Data Curation, Writing – Original Draft, Visualization; **Ferry Santoso:** Funding Acquisition, Writing – Review and Editing, Supervision; **Widya Dwi Aryati:** Writing – Review and Editing, Supervision; **Kunal Nepali:** Writing – Review and Editing, Supervision; **Willy Tirza Eden:** Funding Acquisition, Writing – Review and Editing, Supervision

References

[1] WT Eden, N Solekah, I Nufus, MEP Lestari and PD Palupi. The effect of nanoencapsulation effervescent powder of jengkol peel (Pithecellobium jiringa) in the alloxan-induced diabetic mice. *AIP Conference Proceedings* 2023; **2614**, 030018.

[2] SA Antar, NA Ashour, M Sharaky, M Khattab, NA Ashour, RT Zaid, EJ Roh, A Elkamhawy and AA Al-Karmalawy. Diabetes mellitus: Classification, mediators, and complications; A gate to identify potential targets for the development of new effective treatments. *Biomedicine & Pharmacotherapy = Biomedecine & Pharmacotherapie* 2023; **168**, 115734.

[3] TM Belete. A recent achievement in the discovery and development of novel targets for the treatment of type-2 diabetes mellitus. *Journal of Experimental Pharmacology* 2020; **12**, 1-15.

[4] L Agius. New hepatic targets for glycaemic control in diabetes. *Best Practice and Research in Clinical Endocrinology and Metabolism* 2007; **21(4)**, 587-605.

[5] G Charpentier. Oral combination therapy for type 2 diabetes. *Diabetes/metabolism Research and Reviews* 2002; **18**, S70-S76.

[6] J Lee, S Noh, S Lim and B Kim. Plant extracts for type 2 diabetes: From traditional medicine to modern drug discovery. A*ntioxidants* 2021; **10(1)**, 81.

[7] WT Eden, S Wahyuono, E Cahyono and P Astuti. Phytochemical, antioxidant, and cytotoxic activity of water hyacinth (eichhornia crassipes) ethanol extract. *Tropical Journal of Natural Product Research* 2023; **7(8)**, 3606-3612.

[8] M Azam, WT Eden, AI Fibriana and SR Rahayu. Antioxidant properties of capsule dosage form

from mixed extracts of garcinia mangostana rind and solanum lycopersicum fruit. *Acta Pharmaceutica Sciencia* 2021; **59(1)**, 69-80.

[9] PP Dutta, K Marbaniang, S Sen, BK Dey and NC Talukdar. A review on phytochemistry of Paederia foetida Linn. *Phytomedicine Plus* 2023; **3(1)**, 100411.

[10] MP Borgohain, L Chowdhury, S Ahmed, N Bolshette, K Devasani, TJ Das, A Mohapatra and M Lahkar. Renoprotective and antioxidative effects of methanolic Paederia foetida leaf extract on experimental diabetic nephropathy in rats. *Journal of Ethnopharmacology* 2017; **198**, 451-459.

[11] K Makrilakis. The role of dpp-4 inhibitors in the treatment algorithm of type 2 diabetes mellitus: When to select, what to expect. *International Journal of Environmental Research and Public Health* 2019; **16(15)**, 2720.

[12] S Kalra. Sodium glucose Co-Transporter-2 (SGLT2) inhibitors: A review of their basic and clinical pharmacology. *Diabetes Therapy: Research, Treatment and Education of Diabetes and Related Disorders* 2014; **5(2)**, 355-366.

[13] RD Bongard, M Lepley, K Thakur, MR Talipov, J Nayak, RAJ Lipinski, C Bohl, N Sweeney, R Ramchandran, R Rathore and DS Sem. Serendipitous discovery of light-induced (In Situ) formation of an Azo-bridged dimeric sulfonated naphthol as a potent PTP1B inhibitor. *BMC Biochemistry* 2017; **18(1)**, 10.

[14] MAB Macalalad and AA Gonzales. *In Silico* screening and identification of antidiabetic inhibitors sourced from phytochemicals of philippine plants against four protein targets of diabetes (PTP1B, DPP-4, SGLT-2, and FBPase). *Molecules* 2023; **28(14)**, 5301.

[15] Chemaxon. *Marvin 2025*. Chemaxon, Switzerland, 2025.

[16] NO Boyle, M Banck, CA James, C Morley, T Vandermeersch and GR Hutchison. Open babel: An open chemical toolbox. *Journal of Cheminformatics* 2011; **3**, 33.

[17] GM Morris, R Huey, W Lindstrom, MF Sanner, RK Belew, DS Goodsell and AJ Olson. Software news and updates autodock4 and autodocktools4: Automated docking with selective receptor flexibility. *Journal of Computational Chemistry* 2009; **30(16)**, 2785-2791.

[18] MRF Pratama and S Siswandono. Number of runs variations on autodock4 do not have a significant effect on RMSD from docking results. *Pharmacy & Pharmacology* 2020; **8(6)**, 476-480.

[19] Y. Liu, X Hu, E Li, Y Fang, H Xue, J Zhang, R Jha and R Wang. Bioaffinity ultrafiltration combined with UPLC-ESI-QTrap-MS/MS for screening of xanthine oxidase inhibitors from Paederia foetida L. leaves. *Arabian Journal of Chemistry* 2024; **17(4)**, 105706.

[20] G Xiong, Z Wu, J Yi, L Fu, Z Yang, C Hsieh, M Yin, X Zeng, C Wu, A Lu, X Chen, T Hou and D Cao. ADMETlab 2.0: An integrated online platform for accurate and comprehensive predictions of ADMET properties. *Nucleic Acids Researchvol* 2021; **49**, W5-W14.

[21] R Liu, C Mathieu, J Berthelet, W Zhang, JM Dupret and FR Lima. Human Protein Tyrosine Phosphatase 1B (PTP1B): From structure to clinical inhibitor perspectives. *International Journal of Molecular Sciences* 2022; **23(13)**, 7027.

[22] PJ Ala, L Gonneville, M Hillman, M Becker-Pasha, EW Yue, B Douty, B Wayland, P Polam, ML Crawley, E McLaughlin, RB Sparks, B Glass, A Takvorian, AP Combs, TC Burn, GF Hollis and R Wynn. Structural insights into the design of nonpeptidic isothiazolidinone- containing inhibitors of protein-tyrosine phosphatase 1B. *Journal of Biological Chemistry* 2006; **281(49)**, 38013-38021

[23] YA Puius, YU Zhao, M Sullivan, DS Lawrence, SC Almo and ZY Zhang. Identification of a second aryl phosphate-binding site in protein-tyrosine phosphatase 1B: A paradigm for inhibitor design. *Proceedings of the National Academy of Sciences of the United States of America* 1997; **94(25)**, 13420-13425.

[24] SQ Pantaleão, EA Philot, PTD Resende-Lara, AN Lima, D Perahia, MA Miteva, AL Scott and KM Honorio. Structural dynamics of DPP-4 and its influence on the projection of bioactive ligands. *Molecules* 2018; **23(2)**, 490.

[25] P Antony, B Baby, A Jobe and R Vijayan. Computational modeling of the interactions between DPP IV and hemorphins. *International Journal of Molecular Sciences* 2024; **25(5)**, 3059.

[26] V Mathur, O Alam, N Siddiqui, M Jha, A Manaithiya, S Bawa, N Sharma, S Alshehri, P Alam and F Shakeel. Insight into structure activity relationship of DPP-4 inhibitors for development of antidiabetic agents. *Molecules* 2023; **28(15)**, 5860.

[27] L Mojica and EGD Mejía. Optimization of enzymatic production of anti-diabetic peptides from black bean (Phaseolus vulgaris L.) proteins,

their characterization and biological potential. *Food & Function* 2016; **7(2)**, 713-727.

[28] H Mamoudou, AH Abdoulaye, NYO Ditchou, JN Olumasai, RMZK Adissa and MAM Mune. Computational investigation of Plectranthus neochilus essential oil phytochemicals interaction with dipeptidyl peptidase 4: A potential avenue for antidiabetic drug discovery. *Current Pharmaceutical Analysis* 2025; **21(3)**, 169-178.

[29] R Grempler, L Thomas, M Eckhardt, F Himmelsbach, A Sauer, DE Sharp, RA Bakker, M Mark, T Klein and P Eickelmann. Empagliflozin, a novel selective sodium glucose cotransporter-2 (SGLT-2) inhibitor: Characterisation and comparison with other SGLT-2 inhibitors. *Diabetes, Obesity & Metabolism* 2012; **14(1)**, 83-90.

[30] WH Abdulaal, MA Bakhrebah, MS Nassar, IA Almazni, WA Almutairi, ZS Natto and AK Khattab. Insights from the molecular docking analysis of SGLT2 and FIMH to combat uropathogenicity. *Bioinformation* 2022; **18(11)**, 1044-1049.

[31] S Heng, KM Harris and ER Kantrowitz. Designing inhibitors against fructose 1,6-bisphosphatase: Exploring natural products for novel inhibitor scaffolds. *European Journal of Medicinal Chemistry* 2010; **45(4)**, 1478-1484.

[32] M Yasir, J Park, ET Han, WS Park, JH Han, YS Kwon, HJ Lee, M Hassan, A Kloczkowski and W Chun. Investigation of flavonoid scaffolds as DAX1 inhibitors against ewing sarcoma through pharmacoinformatic and dynamic simulation studies *International Journal of Molecular Sciences* 2023; **24(11)**, 9332.

[33] K Wu, SH Kwon, X Zhou, C Fuller, X Wang, J Vadgama and Y Wu. Overcoming challenges in small-molecule drug bioavailability: A review of key factors and approaches. International journal of molecular sciences 2024; **25(23)**, 13121.

[34] JTS Coimbra, R Feghali, RP Ribeiro, MJ Ramos and PA Fernandes. The importance of intramolecular hydrogen bonds on the translocation of the small drug piracetam through a lipid bilayer. *RSC Advances* 2021; **11(2)**, 899-908.

[35] D Iacopetta, J Ceramella, A Catalano, E Scali, D Scumaci, M Pellegrino, S Aquaro, C Saturnino and MS Sinicropi. Impact of cytochrome P450 enzymes on the phase i metabolism of drugs. *Applied Sciences* 2023; **13(10)**, 6045.